Hyperuricemia Predisposes to the Onset of Diabetes via Promoting Pancreatic β-Cell Death in Uricase-Deficient Male Mice

Jie Lu,[1,2] Yuwei He,[1] Lingling Cui,[1] Xiaoming Xing,[3] Zhen Liu,[1] Xinde Li,[1] Hui Zhang,[2] Hailong Li,[2] Wenyan Sun,[2] Aichang Ji,[1] Yao Wang,[1] Huiyong Yin,[4] and Changgui Li[1,2]

Diabetes 2020;69:1149–1163 | https://doi.org/10.2337/db19-0704

Clinical studies have shown a link between hyperuricemia (HU) and diabetes, while the exact effect of soluble serum urate on glucose metabolism remains elusive. This study aims to characterize the glucose metabolic phenotypes and investigate the underlying molecular mechanisms using a novel spontaneous HU mouse model in which the uricase (*Uox*) gene is absent. In an attempt to study the role of HU in glycometabolism, we implemented external stimulation on *Uox* knockout (KO) and wild-type (WT) males with a high-fat diet (HFD) and/or injections of multiple low-dose streptozotocin (MLD-STZ) to provoke the potential role of urate. Notably, while *Uox*-KO mice developed glucose intolerance in the basal condition, no mice spontaneously developed diabetes, even with aging. HFD-fed *Uox*-KO mice manifested similar insulin sensitivity compared with WT controls. HU augmented the existing glycometabolism abnormality induced by MLD-STZ and eventually led to diabetes, as evidenced by the increased random glucose. Reduced β-cell masses and increased terminal deoxynucleotidyl TUNEL-positive β-cells suggested that HU-mediated diabetes was cell death dependent. However, urate-lowering therapy (ULT) cannot ameliorate the diabetes incidence or reverse β-cell apoptosis with significance. ULT displayed a significant therapeutic effect of HU-crystal–associated kidney injury and tubulointerstitial damage in diabetes. Moreover, we present transcriptomic analysis of isolated islets, using *Uox*-KO versus WT mice and streptozotocin-induced diabetic WT (STZ-WT) versus diabetic *Uox*-KO (STZ-KO) mice. Shared differentially expressed genes of HU primacy revealed Stk17β is a possible target gene in HU-related β-cell death. Together, this study suggests that HU accelerates but does not cause diabetes by inhibiting islet β-cell survival.

Hyperuricemia (HU), a metabolic condition characterized by elevated serum urate (SU), is a primary cause of gout. Epidemiological studies have demonstrated the rapid increasing prevalence of HU worldwide in the last decades (1–3). Although some recent studies have highlighted the connection between SU and glucose homeostasis and indicated that each 1 mg/dL increase in SU was accompanied by a 17% increase in the risk of type 2 diabetes (4,5), there is no conclusion of a causal relationship between HU and diabetes. The Mendelian randomization study by Sluijs et al. (6) did not support a causal effect of circulating urate on diabetes onset and thus concluded that urate-lowering therapies (ULTs) may therefore not be beneficial in reducing diabetes risk. Therefore, whether or how SU is involved in disrupting glucose homeostasis remains elusive. Moreover, the investigation of the possible relationship between urate and glucose metabolism has been hindered by the lack of an appropriate animal model.

The etiology of diabetes is multifactorial, including insulin resistance, defective insulin secretion, and loss of β-cell mass through β-cell apoptosis. Adequate insulin secretion from pancreatic β-cells is necessary to maintain blood glucose homeostasis. Notably, the apoptosis and the

[1]Shandong Provincial Key Laboratory of Metabolic Diseases, Qingdao Key Laboratory of Gout, and Department of Endocrinology and Metabolism, the Affiliated Hospital of Qingdao University, Qingdao, China
[2]Institute of Metabolic Diseases, Qingdao University, Qingdao, China
[3]Department of Pathology, the Affiliated Hospital of Qingdao University, Qingdao, China
[4]CAS Key Laboratory of Nutrition, Metabolism and Food Safety, Shanghai Institute of Nutrition and Health, Shanghai Institutes for Biological Sciences (SIBS), Chinese Academy of Sciences (CAS), Shanghai, China

Corresponding author: Jie Lu, 13127006046@163.com, or Changgui Li, lichanggui@medmail.com.cn

Received 17 July 2019 and accepted 23 March 2020

This article contains supplementary material online at https://doi.org/10.2337/db20-4567/suppl.12030522.

J.L., Y.H., and L.C. contributed equally to this article.

subsequent loss of function of pancreatic β-cells is the major contributor to the progression of diabetes. Although the relationship between HU and diabetes has been implicated, the molecular underpinnings of diabetic β-cell apoptosis promoted by HU remain poorly understood. One piece of evidences from Jia et al. (7) demonstrated that soluble urate can directly cause β-cell death and dysfunction by activation of the nuclear factor-κB–inducible nitric oxide synthase–nitric oxide (NF-κB–iNOS–NO) signal axis in vitro. Thus, understanding the mechanisms of β-cell survival in basal or stress conditions associated with HU is imperative for creating new strategies to prevent and manage diabetes, especially for HU individuals.

Uricase (*Uox*) expressed in rodents can further degrade uric acid into allantoin (8), which has hindered the establishment of suitable rodent models for HU (9). We previously established a spontaneous HU mouse model with *Uox* gene deficiency that is characterized by long-term stable SU levels (7–9 mg/dL) (10). This animal model lays a foundation for further glycometabolism investigations. In the current study, we address the following questions: *1*) whether the *Uox*-KO mouse develops spontaneous glucose abnormities (such as insulin resistance, compromised β-cell functions) and even diabetes, *2*) whether HU imposes stresses on glucose phenotypes or pancreatic β-cells with additional high-fat diet (HFD) and/or streptozotocin (STZ) stimulation in the *Uox* gene-deficiency mouse model, and *3*) how urate works in mouse isolated islets if we have evidence that urate attacks pancreatic β-cells.

RESEARCH DESIGN AND METHODS

Animals

Uox knockout (KO) mice and their wild-type (WT) counterparts (C57BL/6J background) were generated as previously described (10). Briefly, a region of 28 base pairs in exon 3 of the *Uox* gene was deleted using the transcription activator-like effector nuclease technique. The animals were maintained in a temperature-controlled room (22°C), with humidity at 55%, and on a 12-h light-dark cycle (lights on from 7:00 A.M. to 7:00 P.M.) under specific pathogen-free conditions. After a 2-week acclimation period, 8-week-old mice were randomly assigned to two groups (1:1) and fed with an HFD (45% total fat, 35% protein, and 20% carbohydrate) or a regular chow diet ad libitum with free access to water for 20 weeks.

To provoke the potential role of urate in animals, we fed mice the HFD (45% fat, 35% protein, and 20% carbohydrate) for 1 week and then injected them with multiple low-dose STZ (MLD-STZ, 40 mg/kg body wt i.p.) daily for 5 consecutive days. Specifically, STZ was freshly dissolved in 0.1 mol/L citrate buffer (pH 4.5). For comparison, mice were administered STZ and fed a normal diet. Random-fed (9:00–10:00 A.M.) blood glucose levels were determined by glucometer (ACCU-CHEK Inform; Roche Pharmaceuticals). To evaluate the effect of ULT, pegloticase (also known as Krystexxa or Puricase), purchased from Horizon Pharma, was administrated to mice by tail vein injection at a dose of 0.5 mg/kg, with the first injection on the first day of the MLD-STZ intervention, and the second injection was on the 10th day of the MLD-STZ intervention.

Male mice were used for all studies shown, and the age of mice is indicated in the figures. This study was approved by the Affiliated Hospital of Qingdao University Animal Research Ethics Committee.

Blood Biochemistry

Mice were fasted overnight before serum biochemical tests. Blood was collected from the outer canthus the next morning. SU levels were measured immediately from the serum of anesthetized breathing mice (11), using an automatic biochemical analyzer (Toshiba, Tokyo, Japan). Serum creatinine levels and lipid profiles, including total cholesterol (TC), triglycerides (TG), and HDL and LDL cholesterol were assessed by the automatic biochemical analyzer (Toshiba) as well. Blood glucose levels were monitored by tail bleeding with a glucometer (ACCU-CHEK Inform). Diabetes was defined as a random blood glucose of $\geq$16.7 mmol/L (12).

Glucose Tolerance Test, Insulin Tolerance Test, and Glucose-Stimulated Insulin Secretion

Mice were fasted for 8 h before a glucose tolerance test (GTT) or insulin tolerance test (ITT) and then injected with D-glucose at 2 g/kg body wt i.p. or 1 unit/kg insulin (Humulin R; Eli Lilly). Blood was collected at predetermined times (0, 15, 30, 60, and 120 min) after the glucose injection, and the blood glucose levels were determined using a glucometer (ACCU-CHEK Inform).

Glucose-stimulated insulin secretion (GSIS) testing in vivo and in vitro was performed. Briefly, mice were fasted for 8 h and injected with 2 g/kg D-glucose i.p., and serum insulin levels were tested at 0, 15, 30, and 60 min for in vivo GSIS. For in vitro GSIS, isolated islets were purified and harvested by handpicking under a stereomicroscope as described below. The islets (10 per well) were seeded in 24-well plates and then cultured in complete RPMI 1640 (Gibco, Life Technologies) with 10% FBS (HyClone; GE Healthcare, Little Chalfont, U.K.) in 5% CO_2 at 37°C overnight. After incubation for 1 h in glucose-free Krebs buffer (115 mmol/L NaCl, 4.7 mmol/L KCl, 1.2 mmol/L $MgSO_4$, 1.2 mmol/L KH_2PO_4, 20 mmol/L $NaHCO_3$, 16 mmol/L HEPES, 2.56 mmol/L $CaCl_2$, and 0.2% BSA), the islets were treated for 1 h in Krebs buffer with low (3.3 mmol/L) or high (16.7 mmol/L) concentrations of glucose. After treatment, the supernatants were obtained for determination of insulin concentration with an ultrasensitive ELISA kit (ALPCO Diagnostics, Salem, NH).

Pathology Analysis

Mice were sacrificed to extract their pancreas for the pathology analysis. The pancreas was immediately dissected, weighed, and fixed in 10% formalin on ice for 30 min, followed by paraffin embedding of 5-μm serial sections. Tissue serial sections were stained by hematoxylin-eosin (HE) and separately incubated with anti-insulin (1:200) (ab7842; Abcam) rabbit polyclonal antibodies for immunohistochemistry. Primary islet apoptosis was

analyzed by the terminal deoxynucleotidyl TUNEL technique according to the manufacturer's instructions (catalog no. 11684795910; Roche). The samples were stained with DAPI to visualize total cells. Pancreatic sections were also immunostained with anti-insulin antibody to identify β-cells. β-Cell fractional area was determined by quantifying the percentage of insulin-positive pancreas area as a total of the full pancreas area for each section, followed by averaging of six sections per mouse. Images were analyzed using the Pannoramic Digital Slide Scanner. The insulin-positive areas were analyzed by Image-Pro Plus 6 software. β-Cell mass was calculated by multiplying the β-cell fractional area with the initial pancreatic wet weight.

The kidneys were removed, fixed in 10% formalin, embedded in paraffin, and then cut into 4-μm sections. The sections were used for HE, periodic acid Schiff–methenamine (PASM) staining, and periodic acid Schiff (PAS) staining. The percentage of tubule injuries was assessed by scoring six renal cortical tubule sections in randomly selected fields for each group. The glomerulosclerosis index (GSI) was calculated as $[(1 \times N1) + (2 \times N2) + (3 \times N3) + (4 \times N4)]/(N0 + N1 + N2 + N3 + N4)$, where *N*x was the number of glomeruli with each given score (0 for normal glomeruli, 1 for up to 25% involvement, 2 for up to 50% involvement, 3 for up to 75% involvement, and 4 for >75% sclerosis). The average GSI was analyzed based on three given PAS staining sections for each group. Renal crystal sections were obtained from absolute ethanol-fixed kidneys to detect urate crystals under polarized light. The urate crystal areas in each group were calculated by the Image-Pro Plus 6.0 system.

Islets Isolation

Pancreatic islets were isolated from mice with digestive enzyme (13,14). Briefly, a mouse was euthanized with CO_2, followed by cervical dislocation, and then placed supine under a stereomicroscope, with the abdomen cleaned with 75% ethanol. A laparotomy was performed by cutting the skin and the muscular tissue of the thorax with a V-incision from the pubic region up to the diaphragm to expose the abdominal cavity. The common bile duct close to the duodenum was ligated for the retrograde puncture of the common bile duct, followed by a slow perfusion of 3 mL prechilled collagenase IV (catalog no. C5138*S*; Sigma-Aldrich) at 0.5 mg/mL concentration (dissolved in Hanks' balanced salt solution) to fully expand the pancreatic body and tail. The pancreas was then excised and digested at 37°C for 11 min. Islets were purified in Histopaque-1077 (catalog no. 10771; Sigma-Aldrich) by vortexing gently for several seconds.

Microarrays

RNA Isolation and Quantification

Isolated islets from mice were prepared for the following RNA extraction. Briefly, total RNA was extracted and purified using RNeasy Micro Kit (catalog no. 74004; QIAGEN), following the manufacturer's instructions, and checked for a registrant identification number to inspect RNA integration by an Agilent Bioanalyzer 2100 (Agilent Technologies). Only those samples with a 260 nm–to–280 nm ratio between 1.8 and 2.1, a 28*S*-to-18*S* ratio within 1.5 and 2.0, and gel electrophoresis that showed clear 28*S* and 18*S* bands and a weak 5*S* strip were further processed.

Library Preparation

Total RNA samples (100–1,000 ng) were polyA enriched, reverse-transcribed into double-stranded cDNA, and then labeled by Low Input Quick Amp Labeling Kit (catalog no. 5190-2305; One-Color; Agilent Technologies) following the manufacturer's instructions. Each slide was hybridized with 600 ng Cy3-labeled cRNA using the Gene Expression Hybridization Kit (catalog no. 5188-5242; Agilent Technologies) in a hybridization oven. Microarray was performed on Agilent platform using Agilent SurePrint G3 Mouse Gene Expression Microarray 8 × 60K chips (Agilent Technologies).

Data Analysis

Data were extracted with Feature Extraction 10.7 software (Agilent Technologies). We used a cutoff of normalized array values (log2-transformed values >2.0 or <0.5) for islet tissue transcripts. Raw data were normalized by quantile algorithm. Limma and agilp packages were loaded in R 3.4.1 software.

Statistical Analysis

All experimental statistical analyses were performed using GraphPad Prism 8 software (GraphPad). For two-group comparisons, the Student *t* test was used. For multiple comparisons, one-way ANOVA, followed by a Dunnett test, was used to compare each group versus a vehicle-treated group. Data are presented as mean ± SEM. Differences with $P < 0.05$ were considered statistically significant.

Data and Resource Availability

The data discussed in this publication have been deposited in the National Center for Biotechnology Information Gene Expression Omnibus and are accessible through GEO Series accession number GSE142421 (https://www.ncbi.nlm.nih.gov/geo/query/acc.cgi?acc=GSE142421).

RESULTS

Uox-KO Mice Develop Glucose Intolerance but Not Diabetes

In our previous study, we successfully established the mouse model with *Uox* gene (which is mainly expressed in liver) (Supplementary Fig. 1) deficiency to mimic human HU (10). Shown in Fig. 1*A*, SU levels in *Uox*-KO male mice were dramatically increased compared with WT mice ($P < 0.001$) and stabilized at elevated levels (7–9 mg/dL) from 8 to 56 weeks of age. No difference in body weight was observed between age-matched *Uox*-KO and WT mice (Fig. 1*B*). HU did not alter fasting blood glucose or plasma insulin levels even with aging (from 8 to 56 weeks) (Fig. 1*C* and *D*). As for lipid profiles, no difference was shown in TC or HDL and LDL cholesterol between *Uox*-KO males and

their WT counterparts, whereas TG were significantly lower in *Uox*-KO mice compared with WT mice at each age point ($P < 0.001$ at 8 weeks, 24 weeks, and 56 weeks) (Fig. 1*E–H*).

GTT and ITT were performed in mice to further assess the impact of HU on glucose homeostasis. In basal condition, *Uox*-KO males showed a significant impairment in glucose tolerance, indicated by remarkable elevated blood glucose concentrations at 15 and 30 min after 2 g/kg glucose administration at 8 and 24 weeks of age (Fig. 2*A* and *B*) and at 30 min when they were 56 weeks old (Fig. 2*C*). ITT revealed no insulin resistance in *Uox*-KO males, even with prolonged HU stress (Fig. 2*D–F*). These data show *Uox*-KO male mice do not develop diabetes spontaneously though with aging.

HU Does Not Impair Insulin Sensitivity in HFD-Fed Mice

We fed *Uox*-KO male mice and the control WT littermates with the HFD or the normal chow diet, starting at 8 weeks of age, and continued for 20 weeks. Both genotypes displayed comparable SU levels and circulating lipids (including TC and HDL and LDL cholesterol) before and after the experimental feeding (Table 1). The HFD elevated TC, TG, and LDL cholesterol and decreased HDL cholesterol in both genotypes (Table 1). After 20 weeks of exposure to the HFD, the WT mice showed increased body weight compared with the *Uox*-KO mice (Table 1). Although plasma insulin levels displayed a significant elevation in HFD-fed WT mice compared with chow diet–fed mice, the HFD-fed *Uox*-KO mice showed a dramatic reduction in plasma insulin levels compared with the HFD-fed WT mice (Table 1). This result indicates a failure of compensatory insulin production by pancreatic β-cells in *Uox*-KO mice.

We also performed GTT and quantified the area under the curve (AUC) that integrates the values from 0 to 120 min of GTT. After 20 weeks of being fed with the chow diet or HFD, blood glucose in WT and *Uox*-KO male mice was restored to normal concentrations at 120 min after the glucose challenge (Fig. 3*A*), despite that a higher peak at the 30-min point was observed in HFD-fed *Uox*-KO mice. However, after 20 weeks of being fed the HFD, both genotypes exhibited a retarded glucose clearance compared with mice fed the normal chow diet (Fig. 3*A*). Remarkably, the blood glucose levels in HFD-fed *Uox*-KO mice were sustained at a dramatically higher level over the whole course of GTT compared with HFD-fed WT controls (Fig. 3*A*), resulting in a significant increase in the AUC of the GTT (Fig. 3*B*) and indicative of severe glucose intolerance.

The development of glucose dysmetabolism is ultimately attributable to impaired insulin action or insufficient insulin production, or both. To clarify whether insulin resistance accounts for the glycol-metabolic disorders in HFD-fed *Uox*-KO mice, we used an ITT. Compared with the chow diet, the disappearance of glucose after the insulin challenge was comparable by the HFD (Fig. 3*C*), displaying no insulin resistance in diet-induced *Uox*-KO male mice. The AUC of the ITT was comparable between HFD-fed WT and *Uox*-KO mice as well (Fig. 3*D*), suggesting an equivalent degree of insulin resistance in the two genotypes.

Islet function was determined by in vivo and in vitro GSIS. Similar to the results of *Uox*-KO mice islet function in our previous study (10), HFD-fed *Uox*-KO mice secreted a significantly lower amount of insulin at 15 and 30 min (Fig. 3*E*), consistent with the GTT results above. Although isolated islets derived from HFD-fed *Uox*-KO mice secreted a similar amount of insulin as HFD-fed WT islets at low glucose concentration (3.3 mmol/L), insulin secretion was decreased by 22.6% in HFD-fed *Uox*-KO islets at a high glucose concentration (16.7 mmol/L), as shown in Fig. 3*F*. Collectively, these data suggest that HU impairs GSIS in HFD-fed *Uox*-deficient males, contributing to increased glucose intolerance.

HU Induces Diabetes With External MLD-STZ Stimulation

Given HU compromised β-cell functions and impaired glucose tolerance, we suppose urate worsens hyperglycemia in an established model of diabetes induced by HFD + MLD-STZ (40 mg/kg/day for 5 days). Pegloticase, an approved recombinant porcine-like uricase drug, was indicated for the treatment of HU mice. As indicated by Fig. 4*A*, the random glucose levels in STZ-induced diabetic *Uox*-KO (STZ-KO) mice elevated markedly on day 7, and then severe hyperglycemia developed, which over time resulted in uncontrolled diabetes (day 0 vs. day 7, $P < 0.01$; day 0 vs. day 8–20, $P < 0.001$), whereas the STZ-induced diabetic WT (STZ-WT) mice showed stable glucose levels on the first 8 days ($P > 0.05$) and were significantly elevated afterward ($P < 0.01$). Consistent with the previous reports, a low dose of STZ enhanced random glucose, and 23.1% of the mice developed diabetes. However, 87.5% of the STZ-KO mice exhibited average random blood glucose levels >16.7 mmol/L on day 11 and afterward (Fig. 4*B*). ULT lowered the diabetes incidence, although without a significant difference, and ultimately reached 75.0% in STZ-KO mice (Fig. 4*B*). Furthermore, ULT delayed the diabetes onset from day 7 to day 10 (Fig. 4*B*). Therefore, MLD-STZ stimuli could accelerate the development of diabetes, and ULT can only partially reverse this deterioration in STZ-KO males.

HU-Related Diabetes Is Manifested by Increased β-Cell Apoptosis

For determination of whether impaired glucose intolerance was caused by a reduction in β-cell number and islet mass, we extracted mice pancreas tissues for further analysis. No apparent histological lesions, stained with HE or with antibodies against insulin, were detected in the pancreatic islets of the *Uox*-KO males and controls (Fig. 5*A* and *B*). Pancreatic sections were coimmunostained with anti-insulin antibody to visualize β-cells. Compared with the control groups, pancreatic insulin content was lower in STZ-KO mice than in control mice (Fig. 5*A* and *B*). Accordingly, relative β-cell mass,

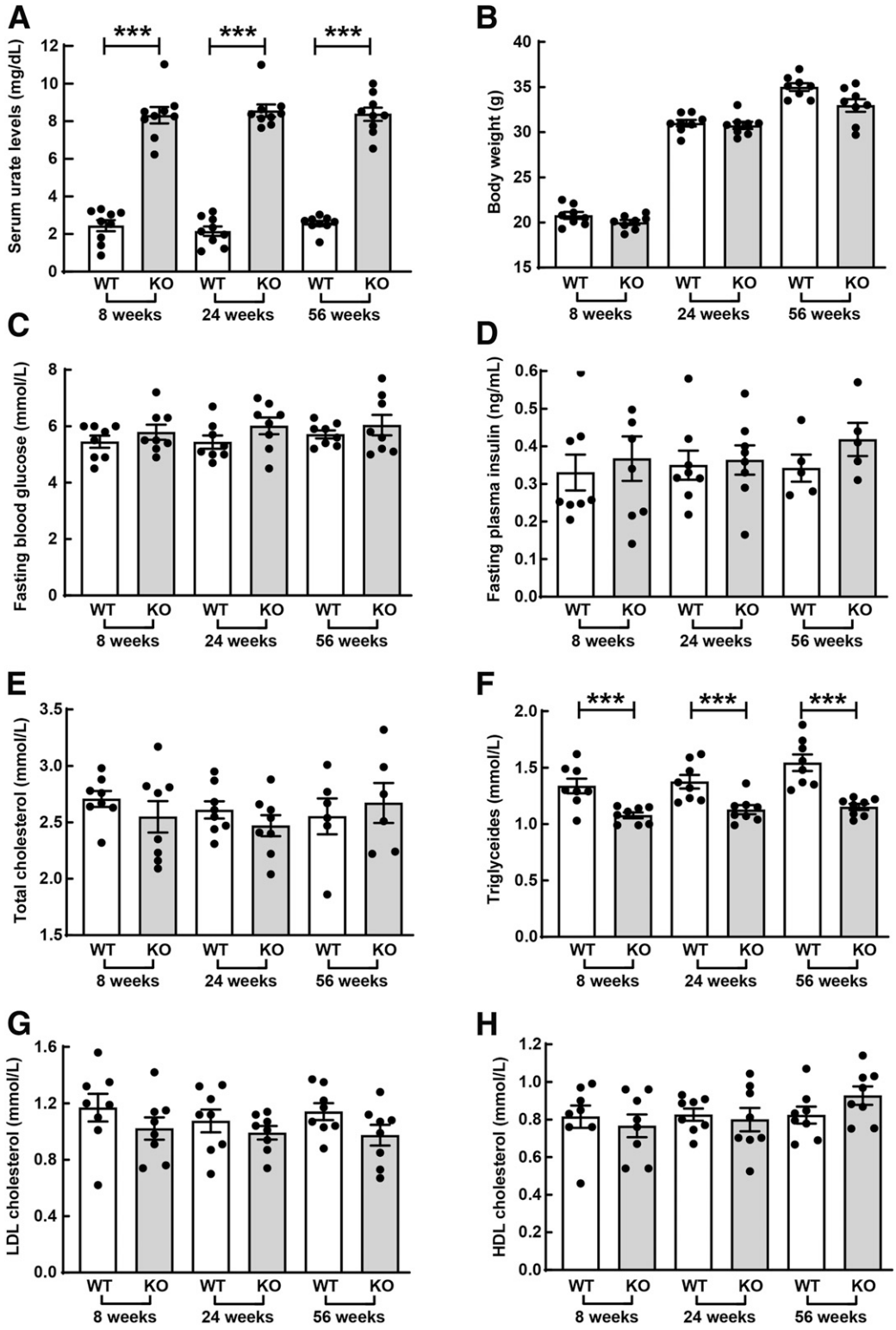

Figure 1—General characteristics of *Uox*-KO male mice and WT counterparts stratified by age. *A*: SU levels were measured at the age of 8, 24, and 56 weeks in KO and WT mice ($n = 9$). *B*: Body weights were evaluated accordingly ($n = 8$). Fasting blood glucose (*C*) and fasting plasma insulin (*D*) were detected ($n = 5$–8). Lipid profiles, including TC (*E*), TG (*F*), LDL cholesterol (*G*), and HDL cholesterol (*H*) were determined in 8-, 24-, and 56-week-old mice ($n = 6$–8). ***$P < 0.001$. Data are expressed as mean ± SEM.

determined by insulin immunoreactivity, was 62% lower in STZ-KO mice (Fig. 5*A* and *B*). To determine whether cell death contributes to reduced β-cell mass in STZ-KO mice, we measured islet apoptosis by TUNEL staining. The number of TUNEL-positive β-cells was higher in STZ-KO mice than in control mice (Fig. 5*C* and *D*),

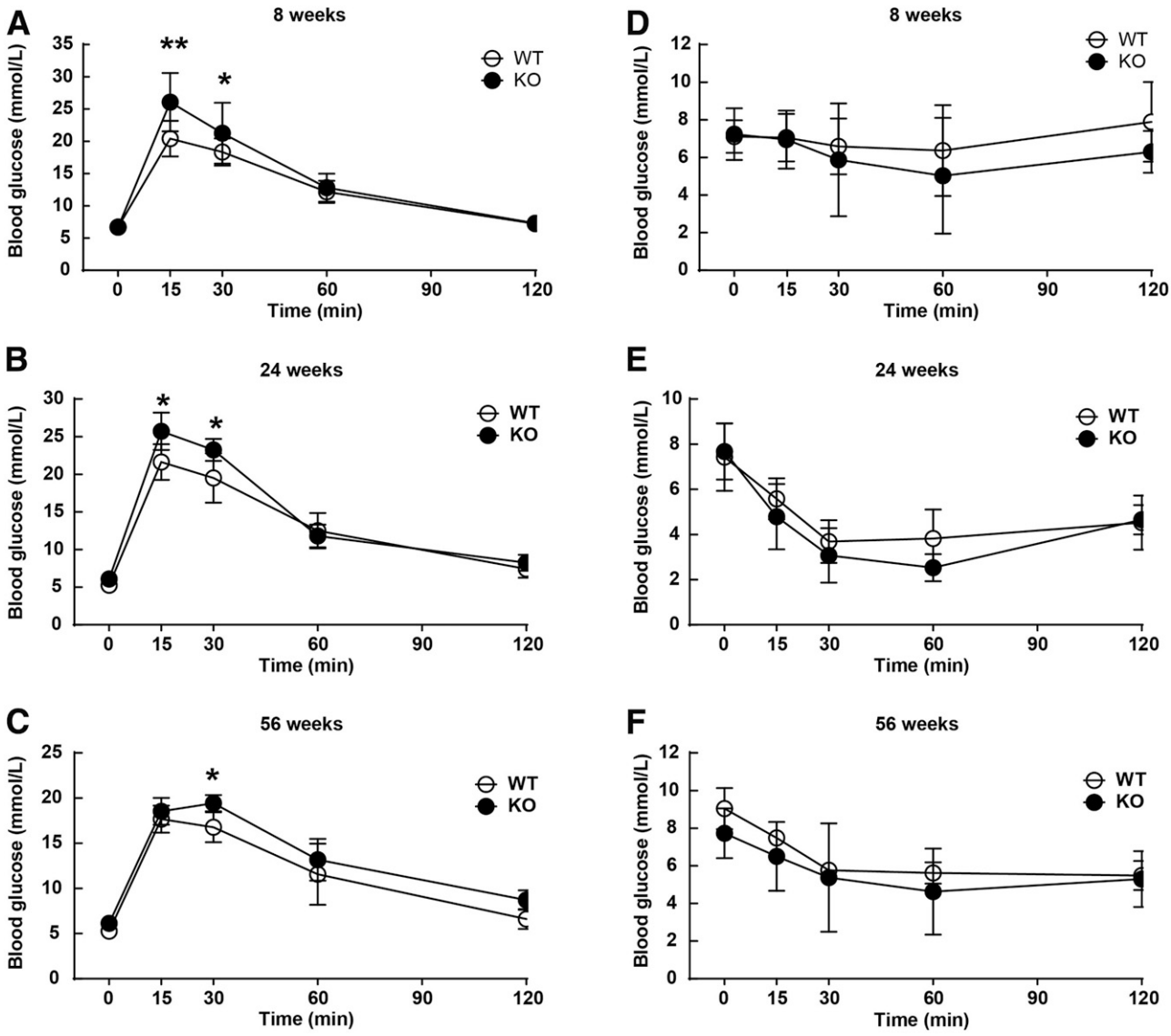

Figure 2—HU impairs glucose tolerance in *Uox*-KO male mice. GTT were performed in *Uox*-KO mice and WT controls with a 2 g/kg glucose i.p. injection after 8 h fasting at the age of 8 weeks (*A*), 24 weeks (*B*), and 56 weeks (*C*), separately ($n = 6$). *D–F*: Insulin (1 unit/kg) was administrated i.p. after 8 h fasting for ITT in 8-, 24-, and 56-week-old mice ($n = 6$). $^{*}P < 0.05$, $^{**}P < 0.01$. Data are expressed as mean ± SEM.

tending to a 42% increase (Fig. 5*C* and *D*). This finding suggests HU promotes not only the loss of β-cell mass but also apoptosis of the pancreatic β-cell in STZ-KO mice. These morphological alterations are consistent with the changes in plasma insulin levels, indicating that β-cell apoptosis chiefly contributes to the onset of diabetes in STZ-KO males.

We next asked whether ULT would be able to reverse the pancreatic β-cell apoptosis with MLD-STZ in HU mice. Shown in Fig. 6*A*, the β-cell masses were significantly smaller in STZ-KO males than in STZ-WT controls ($P < 0.001$). However, the ULT did not reverse the loss of β-cell mass (STZ-KO vs. ULT-KO, $P > 0.05$) (Fig. 6*A*). MLD-STZ exaggerated the islet β-cell death compared between STZ-KO and STZ-WT mice, indicated by TUNEL staining (Fig. 6*B*). Consistently, the number of TUNEL-positive β-cells was significantly higher in STZ-KO mice than in their controls (Fig. 6*C*). However, no significant decreases in TUNEL-positive β-cell signals (Fig. 6*B*) or analysis numbers (STZ-KO vs. ULT-KO, $P > 0.05$) (Fig. 6*C*) were detected after 21 days of ULT in STZ-induced *Uox*-KO mice. Thus, our findings did not support the benefits of ULT on β-cell vitality.

ULT Ameliorates Tubulointerstitial Injury in Diabetes

To evaluate renal changes after STZ stimulation and ULT intervention, we did kidney functional and histological experiments in both genotypes. SU levels were significantly higher in STZ-induced *Uox*-KO male mice than in their WT controls ($P < 0.001$) (Fig. 7*A*). The same results were shown in serum creatinine levels, which are indicators of

Table 1—Body weight and serum biochemical profiles of *Uox*-KO and WT mice after 20 weeks on an HFD or normal chow diet

	WT (n = 8)		KO (n = 8)	
Characteristic	Chow	HFD	Chow	HFD
SU (mg/dL)	2.51 ± 0.24	2.66 ± 0.28	8.58 ± 0.40$^{###}$	8.49 ± 0.55$^{###}$
TC (mmol/L)	2.88 ± 0.08	4.30 ± 0.15**	2.74 ± 0.10	4.05 ± 0.34**
TG (mmol/L)	1.44 ± 0.05	1.85 ± 0.20**	1.13 ± 0.07	1.78 ± 0.30**
LDL cholesterol (mmol/L)	0.94 ± 0.05	1.26 ± 0.19*	1.01 ± 0.08	1.35 ± 0.20*
HDL cholesterol (mmol/L)	0.92 ± 0.04	0.81 ± 0.10*	0.88 ± 0.09	0.73 ± 0.25*
Body weight (g)	32.7 ± 0.66	35.9 ± 0.58***	31.5 ± 0.74	34.1 ± 0.81***$^{##}$
Plasma insulin (ng/mL)	0.53 ± 0.04	0.58 ± 0.04	0.80 ± 0.05$^{#}$	0.32 ± 0.03***$^{##}$

Data are expressed as mean ± SEM. *$P < 0.05$, **$P < 0.01$, ***$P < 0.001$, chow diet vs. HFD; $^{#}P < 0.05$, $^{##}P < 0.01$, $^{###}P < 0.001$, WT vs. KO.

renal function ($P < 0.001$) (Fig. 7*B*). ULT increased renal function in STZ-KO males, displaying significant decreases in SU and creatinine levels ($P < 0.001$) (Fig. 7*A* and *B*).

STZ-KO mice showed dilated Bowman spaces and tubules and collapsed and necrotic nephrons by pathological analysis (Fig. 7*C*). The tubular damage was significantly severe, with tubular dilation, detachment of tubular epithelial cells, and condensation of tubular nuclei appearance in STZ-KO mice (Fig. 7*C*). ULT prevented the development of these lesions indicated by decreased percentage of tubular damage in ULT-KO mice (Fig. 7*D*). PASM staining exhibited obvious glomerular mesangial hyperplasia, increased glomerular matrix, and thickened glomerular basement membrane in diabetic STZ-KO mice compared with their WT controls (Fig. 7*C*). PAS staining documented glomerular mesangial expansion and glomerular sclerosis, early features of diabetic nephropathy, in STZ-KO mice compared with STZ-WT mice (Fig. 7*C*). The GSI, calculated by PAS staining sections, was increased in STZ-KO mice compared with STZ-WT mice ($P < 0.05$) (Fig. 7*E*). However, ULT did not prevent the glomerular injury in STZ-induced HU mice as quantified by GSI (Fig. 7*E*). HU STZ-KO mice showed significant renal urate crystal deposits ($P > 0.05$) (Fig. 7*C*). Crystals were dissolved by ULT in STZ-KO mice with decreased urate crystal areas ($P < 0.001$) (Fig. 7*F*). The histological analysis presented that ULT exhibited a significant therapeutic effect of HU-crystal–associated kidney injury and tubulointerstitial injury manifestation in diabetic nephropathy.

Differentially Expressed Genes in HU and/or Diabetic Mice

We then wondered whether differentially expressed genes (DEGs) in islets of the HU and/or diabetic mice would explain the molecular mechanism of urate on impaired glucose metabolism. Microarray data were represented by heat maps (Fig. 8*A* and *B*) in subgroup comparisons of *Uox*-KO mice versus *Uox*-WT mice and STZ-KO mice versus STZ-WT mice. We selected the genes based on adjusted $P < 0.05$ and absolute fold change >2. In *Uox*-KO versus *Uox*-WT groups, 850 of 2,018 genes were upregulated and 1,168 of 2,018 genes were downregulated (Fig. 8*C*). Whereas in STZ-KO versus STZ-WT groups, 29 of 171 genes were upregulated and 142 of 171 genes were downregulated (Fig. 8*D*). When compared between *Uox*-KO versus *Uox*-WT and STZ-KO versus STZ-WT groups together, one gene (*Stk17β*) was shared in the upregulated DEGs and five genes (*Fut4-ps1*, *Erich3*, *1700027H10Rik*, *Kcnh2*, and *Klhl32*) in the downregulated gene set (Fig. 8*C* and *D*). These shared genes were the urate primacy functioning genes. It is notable that the shared upregulated gene, *Stk17β*, plays a key role in a wide variety of cell death signaling pathways.

DISCUSSION

Whether HU is a causal or noncausal factor for diabetes remains controversial. Although numerous clinical studies have showed that HU predicts the development of diabetes and that the ULT could reduce the diabetes incidence or fasting glucose levels accordingly, the causal relationship between HU and diabetes and related mechanisms remains elusive. The current study firstly demonstrated that HU augmented the existing glycometabolism abnormality induced by MLD-STZ and induced diabetes by promoting not only the loss of β-cell mass but also pancreatic β-cell apoptosis in STZ-induced *Uox*-KO male mice. Although HU increased the incidence of diabetes when accompanied with STZ stimuli, ULT can only ameliorate the incidence by a small proportion without significant statistical differences. In addition, our transcriptomic results indicated that *Stk17β* is a possible target gene in HU-induced β-cell apoptosis.

Multiple lines of evidence have shown the association between HU and diabetes. A community-based study in the U.S. demonstrated the risk of diabetes incidence increased 18% with every 1 mg/dL SU elevation, and the association remained significant after adjustment for fasting glucose and insulin levels (15). The diabetes incidence was 19% for SU ≤7 mg/dL patients, 23% for SU 7 mg/dL to ≤9 mg/dL, and 27% for SU >9 mg/dL in an 80-month follow-up investigation that included 1,923 U.S. veterans (15). This study also indicated ~8.7% of all new cases of diabetes were statistically attributed to HU (15). The age- and

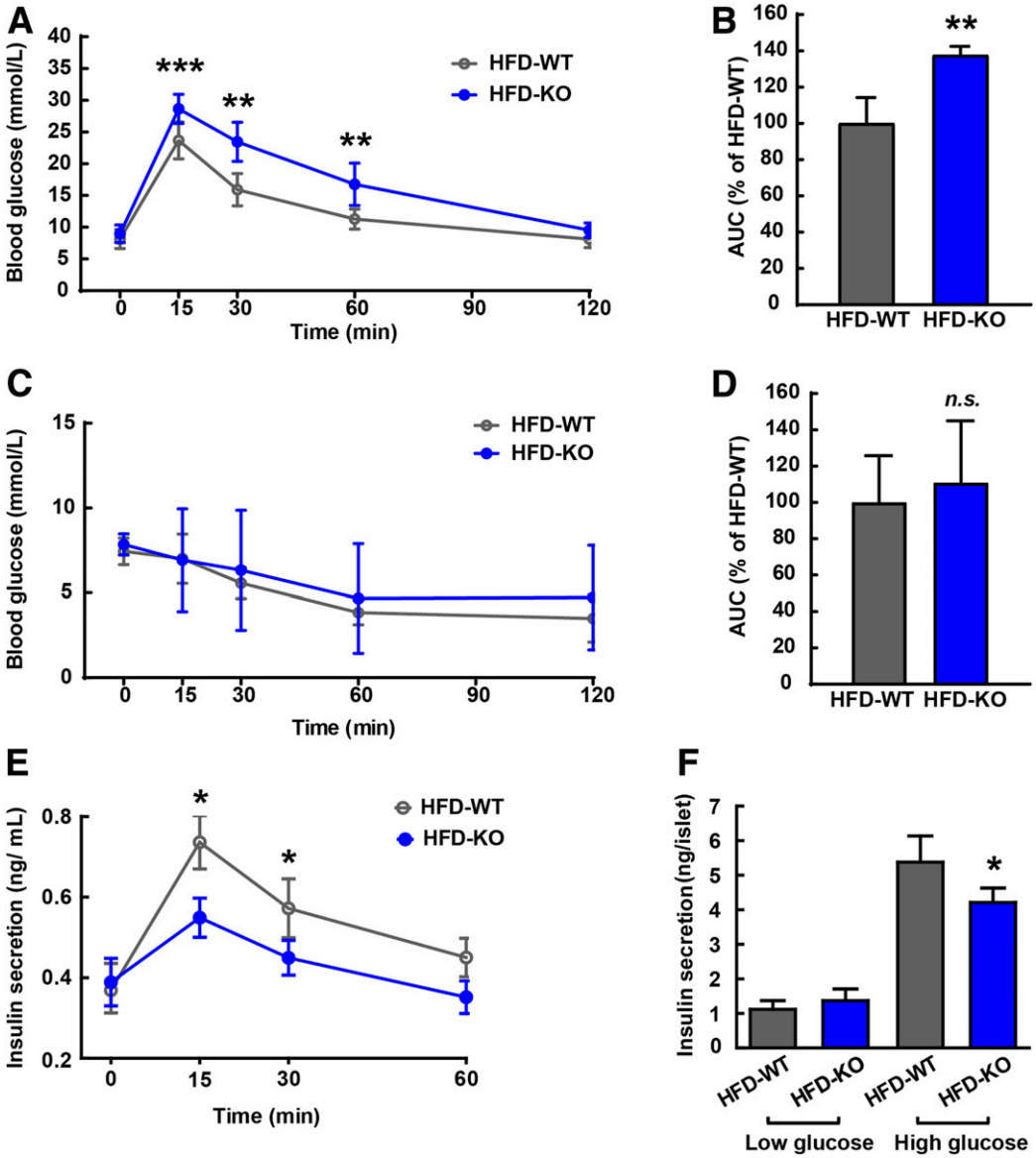

Figure 3—HU strengthens glucose intolerance with HFD stimuli. *A*: GTTs were used for chow diet– and HFD-fed 8-week-old *Uox*-KO male mice and WT controls ($n = 8$). *B*: AUC integrated from the period of 0–120 min was calculated based on the GTT curves. ITTs were monitored (*C*), and corresponding AUCs were determined (8-week-old mice, $n = 8$) (*D*). *E*: Plasma insulin levels were measured with plasma collected at 0, 15, 30, and 60 min after glucose injection (2 g/kg i.p.) in 8-week-old *Uox*-KO mice and WT mice ($n = 6$ in each group). *F*: Supernatant insulin levels were determined after in vitro GSIS with isolated pancreatic β-cells ($n = 6$ in each group). $^*P < 0.05$, $^{**}P < 0.01$, $^{***}P < 0.001$. Data are expressed as mean ± SEM.

sex-adjusted hazard ratio for diabetes was 2.83 for the fourth quartile of SU in subjects from the Rotterdam study (16). Although epidemiology studies showed that HU predicts the development of diabetes, no causality was found in the Mendelian randomization study (6).

Thus, for further phenotype and mechanism explorations, a major obstruction is the lack of an appropriate animal model given that *Uox* in most mammals, including rodents, is functional. Here, we were able to use *Uox*-KO mice to study the potential role of urate in glucose metabolism. Traditional establishment strategies, such as potassium oxonate (a chemical inhibitor of uricase) i.p. injection (17), would interfere with the effects of HU per se as the additional exogenous intervention. An advantage here is that this mouse model is a suitable HU model because of its consistent and stable SU elevations to simulate a human-specific biological background of elevated urate (10).

Next, we further stimulated this spontaneous HU mouse model with the HFD and/or MLD-STZ. A phenotypic heterogeneity in glycometabolism existed between sexes in the *Uox*-KO model, displaying severe glucose intolerance and more sensitivity to STZ in *Uox*-KO males than in females in a previous study (10). To avoid confounding factors due to sex or sex hormone differences, only male mice were used

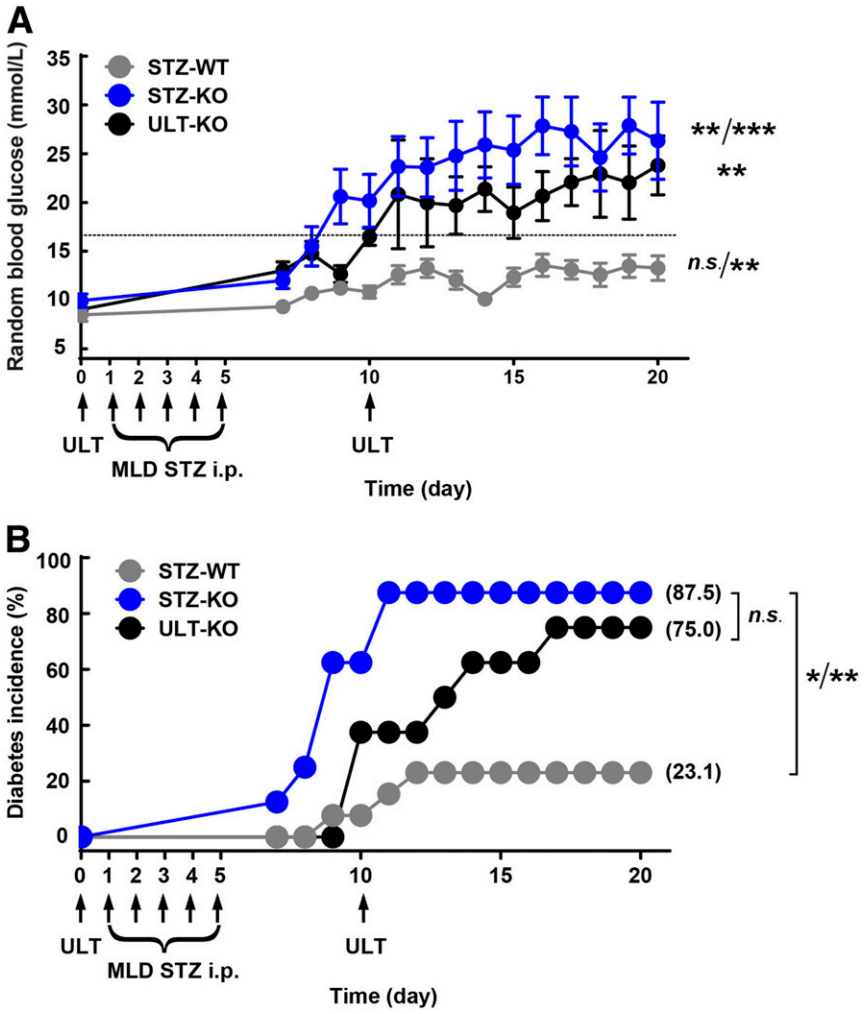

Figure 4—HU induces diabetes with external MLD-STZ stimulation. *A*: Random blood glucose levels were monitored daily after administration of MLD-STZ (40 mg/kg/day for 5 days) for 20 consecutive days (8-week-old mice, $n = 13$, 8, and 8 for STZ-WT mice, STZ-KO mice, and pegloticase therapy ULT-KO mice separately, respectively). *B*: The diabetes incidence in 8-week-old mice was calculated by percentage ($n = 13$, 8, and 8 in each group, respectively). Diabetes was defined as random blood glucose ≥16.7 mmol/L. *P* trend value is presented as $^{*}P < 0.05$, $^{**}P < 0.01$, $^{***}P < 0.001$. Data are expressed as mean ± SEM.

in the current study. Further investigations in female mice would help to delineate a full picture of the effect of HU on glucose metabolism.

Our data show significant elevated blood glucose concentrations at 15 and 30 min of GTT under basal conditions and in response to high-fat feeding (Figs. 2 and 3). Moreover, the plasma insulin drop indicated the compromise of β-cell function is responsible for glucose intolerance. The link of HU and insulin resistance has been extensively reported and discussed (18,19). Spontaneous HU represents one of the metabolic syndromes resulting from the interactions between genetic and environmental factors, including dietary and behavioral factors, which also contribute to insulin resistance in studies (20). Thus, genetically modified HU mouse models lack major complicated genetic or nongenetic risk factors, and HU indeed did not induce insulin resistance, which is normally obesity related. We then fed *Uox*-KO mice and WT controls the HFD or normal chow diet. The results showed HFD-fed *Uox*-KO mice displayed a dramatic reduction in plasma insulin levels compared with HFD-fed WT mice, which indicated a failure of compensatory insulin production by β-cells in the *Uox*-KO mice. Glycol-metabolism evaluations, including GTT, ITT, and GSIS, hint at severe glucose intolerance, with unchanged insulin sensitivity in HFD-induced *Uox*-KO mice (Fig. 3). To be noted, neither the fasting glucose nor fasting insulin changed in the *Uox*-KO mice, even with aging (Fig. 1). In this study, the lack of being able to see a urate-to-insulin resistance relationship is based on the use of a high-fat rather than a high-sugar diet. A similar conclusion was drawn by Kelly and colleagues (21) that systemic HU, while clearly a biomarker of the metabolic abnormalities of obesity, does not appear to be causal. Mendelian randomization studies that focused on genetic variants associated with urate, thereby removing confounding factors such as obesity, showed

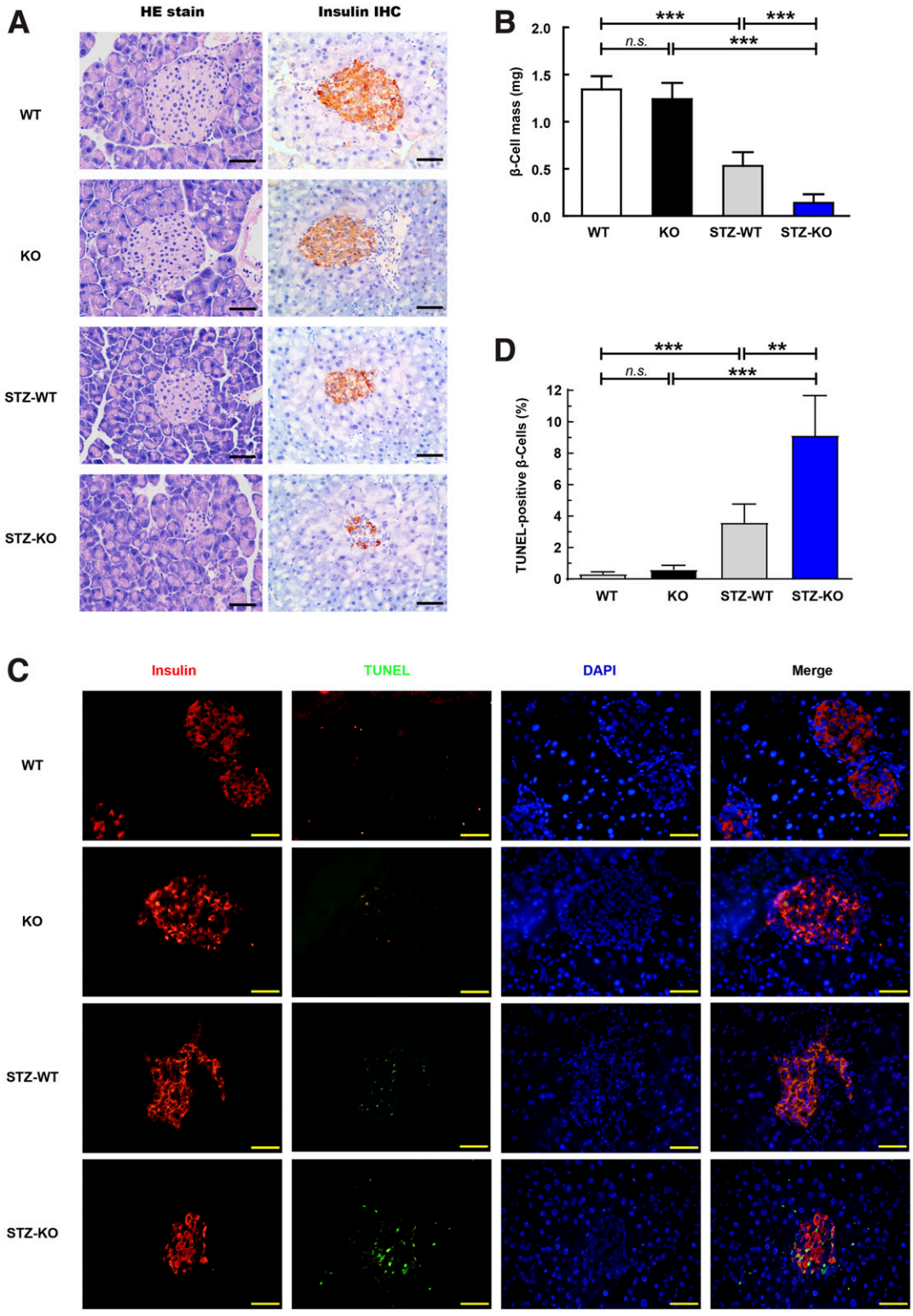

Figure 5—HU causes pancreatic β-cell death under MLD-STZ stimuli. *A*: Pancreatic sections were histologically stained for HE and immunohistochemically (IHC) stained for insulin, respectively (8-week-old mice, $n = 6$). *B*: Total areas of pancreatic tissues and insulin-positive cells were traced manually and determined by counting 10 islets or more in 6 sections per mouse (8-week-old mice, $n = 6$) in each group. β-Cell mass was analyzed, and results are shown in multiplying the β-cell ratio (insulin-positive areas–to–total area) with the initial pancreatic wet weight. *C*: Insulin-positive cell apoptosis was analyzed by the terminal deoxynucleotidyl TUNEL (8-week-old mice, $n = 6$). *D*: Double-positive ratio of insulin and TUNEL was measured in each group (8-week-old mice, $n = 6$). Scale bars = 50 μm. $^{**}P < 0.01$, $^{***}P < 0.001$. Data are expressed as mean ± SEM.

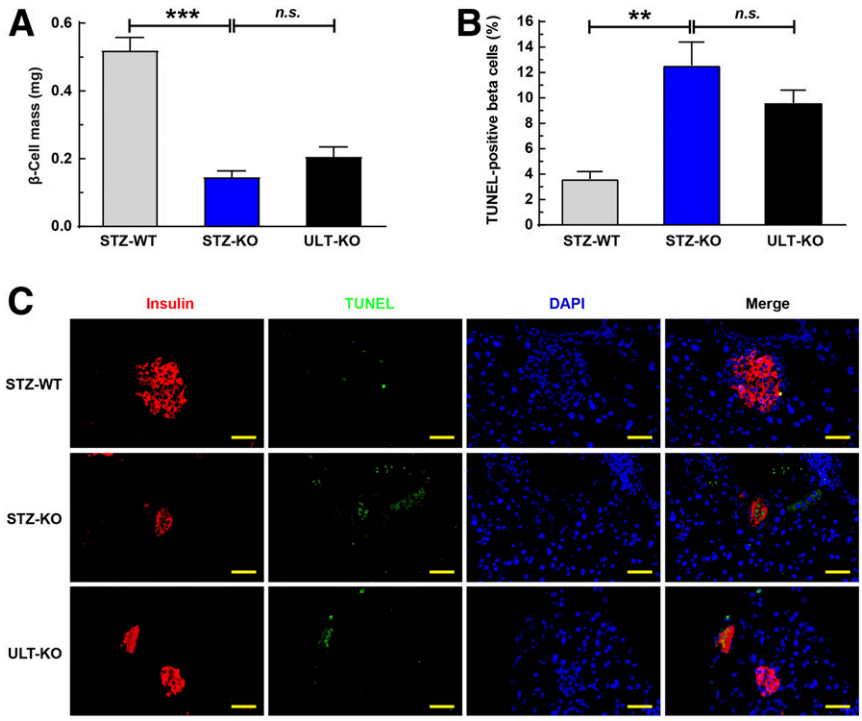

Figure 6—ULT reversed few pancreatic β-cell deaths stimulated by MLD-STZ. Mice were sacrificed on the 21st day after the first MLD-STZ (40 mg/kg/day for 5 days) injection. *A*: β-Cell mass was calculated by multiplying the β-cell ratio (insulin-positive areas–to–total area) with the initial pancreatic wet weight (11-week-old mice, $n = 3$). *B*: Insulin-positive cell apoptosis was analyzed by the terminal deoxynucleotidyl TUNEL (11-week-old mice, $n = 3$). *C*: Double-positive ratio of insulin and TUNEL was measured in each group (11-week-old mice, $n = 3$). Scale bars = 50 μm. $^{**}P < 0.01$, $^{***}P < 0.001$. Data are expressed as mean ± SEM.

elevated urate could not independently predict diabetes development (6,22), which also supports our study findings. However, in models of sugar-/fructose-induced insulin resistance or in models where liver xanthine oxidase activity is increased, then one does see urate-dependent insulin resistance (23,24), which is likely mediated by gluconeogenesis (25). Further investigations using sugar-/fructose-fed *Uox*-KO mice are needed to detect the relationship between urate and insulin resistance.

In the current study, we report that *Uox* deficiency predisposes mice to the onset of diabetes, which results from a loss of β-cell mass under conditions of the HFD accompanied by MLD-STZ. The study has provided both functional and mechanistic data showing the proapoptotic effect of HU in β-cells. This is the first in vivo investigation suggesting a critical role of HU in acceleration of the progression from impaired glucose tolerance into diabetes via the action of promoting β-cell death. Increasing incidence of diabetes is also accompanied by decreased islet area and β-cell mass (Figs. 4 and 5), which corroborates that this glucose intolerance induced by HU is primarily caused by β-cell death. Multiple factors and signaling mechanisms have been demonstrated to influence β-cell compensation, of which β-cell apoptosis has emerged as a key event causing decompensation of β-cells and the development of diabetes (26). Insulin deficiency has been demonstrated to play a causative role in the development of diabetes from both animal and human studies (26). In line with this, *Uox*-KO mice induced by MLD-STZ develop diabetes, accompanied by hypoinsulinemia and increased β-cell apoptosis. The diabetic phenotype of *Uox*-KO mice not only indicates that loss of functional β-cell mass is a key cause of the disease but also reveals a critical role of HU that is required for maintaining β-cell survival in the STZ-induced condition. However, it is worth noting that no differences were found in β-cell mass and insulin production between *Uox*-KO mice and WT controls fed the normal chow diet, suggesting that HU is not required for islet development and is dispensable under nonstressed physiological conditions.

The benefits of ULT are still inconclusive. Randomized trials have reported that ULT by allopurinol improves insulin resistance in asymptomatic HU individuals (27,28), and similar improvement in insulin resistance has been observed with the use of benzbromarone (29). However, in a gout population, the incidence of diabetes was lower in urate-lowering drug (ULD) users than in nonusers (30). In vivo study showed oral administration of ULD dose-dependently reduced the blood glucose level and improved glucose tolerance and insulin resistance in *db*/*db* mice (31). Whether asymptomatic HU should be treated remains controversial, as Sluijs et al. (6) concluded that SU is not causally linked to diabetes and that ULTs may therefore not be beneficial in lowering diabetes risk. A long-held notion in diabetes is that macrophages within

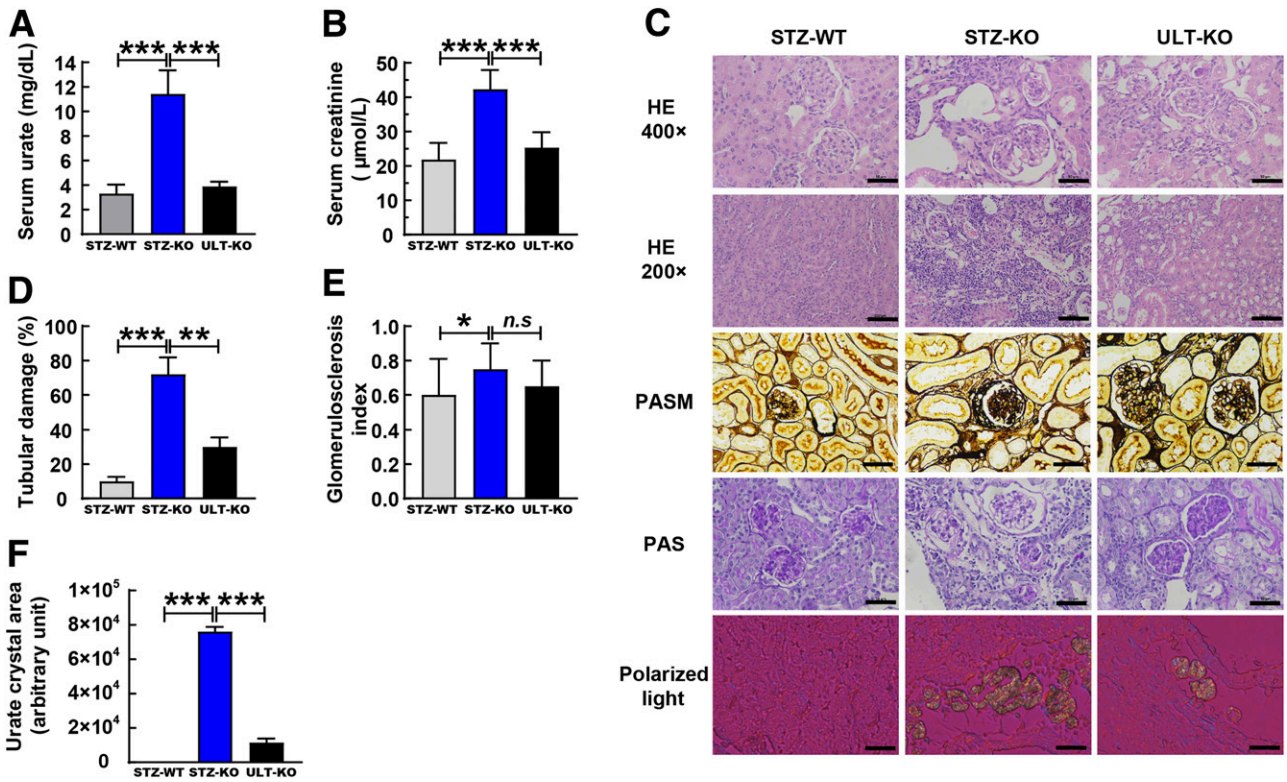

Figure 7—Renal function and pathological changes were evaluated in male 11-week-old mice. *A*: SU levels were measured at the end of experiments ($n = 13$ for WT and $n = 8$ for *Uox*-KO mice in each group). *B*: Serum creatinine levels, indicators of renal function, were determined by the automatic biochemical analyzer ($n = 13$ for WT and $n = 8$ for *Uox*-KO mice in each group). *C*: Renal pathohistology was detected by HE staining, PASM staining, and PAS staining ($n = 6$). Deposits of renal urate crystals were investigated under polarized light ($n = 3$). *D*: Quantification of tubulointerstitial injury. Quantitative analysis for tubulointerstitial injury was assessed by scoring six renal cortical tubule sections (original magnification ×200, HE) in randomly selected fields for each group ($n = 6$). *E*: The GSI was calculated to evaluate diabetic nephropathy based on three given PAS staining sections for each group ($n = 6$). *F*: Urate crystal areas were calculated by the Image-Pro Plus 6.0 system with arbitrary units ($n = 3$). Scale bars = 50 μm in HE (original magnification ×200), PASM, PAS, and polarized light sections. Scale bars = 100 μm in HE (original magnification ×400). $^*P < 0.05$, $^{***}P < 0.001$. Data are expressed as mean ± SEM.

the islet produce reactive oxygen species and proinflammatory cytokines, creating a β-cell cytotoxic environment (32). Pegloticase, a recombinant uricase, exerts its urate-lowering role by degrading urate with a mild oxidative stress. Lowering SU may also reduce oxidative stress because urate, although an antioxidant in noncellular systems, is a pro-oxidant in cellular systems. The present in vivo ULTs exhibited only a partial reverse function on reducing diabetes incidence (Fig. 4) and could not ameliorate β-cell apoptosis (Fig. 6) or glomerular lesions in diabetes (Fig. 7). Substantial short-term ULT did not have a direct protective effect on β-cell apoptosis or antidiabetic potential, suggesting that, on its own, this might not be an effective strategy for restoring β-cell function in STZ-induced HU mice. Longer-term ULT needs to be done in future work to solidify the conclusion.

One of the interesting findings in this study is that ULT improved tubulointerstitial injury but not glomerular lesions in STZ-KO mice. Gilbert and Cooper (33) suggested that tubulointerstitial injury is a major feature of diabetic nephropathy and that its development may reflect influences that are common to other forms of renal disease and also those that are unique to diabetes. An in vivo study showed HU plays a pathogenic role in the mild tubulointerstitial injury associated with diabetic nephropathy but not glomerular damage in diabetic mice (34). Other factors, such as high glucose or oxidative stress, could be responsible for the diabetic glomerular lesion because high glucose is well known to be one of the major stimuli to accelerate extracellular matrix deposition in diabetic glomeruli (35).

Contrary to studies that have previously reported a positive causal association with progression of chronic kidney diseases (CKDs) (36), urate concentration was not causally related to the development of diabetic nephropathy in a Mendelian randomization study by Ahola et al. (37). This Mendelian randomization analysis suggested that the SU concentration does not have any causal effect on diabetic kidney complications but is rather a downstream marker of the kidney damage (37). Moreover, as one Mendelian randomization study suggests that SU is a causal risk factor for CKD in the general population (38), it might be that SU plays a role only in the processes leading to nondiabetic renal disease rather than in pure diabetic

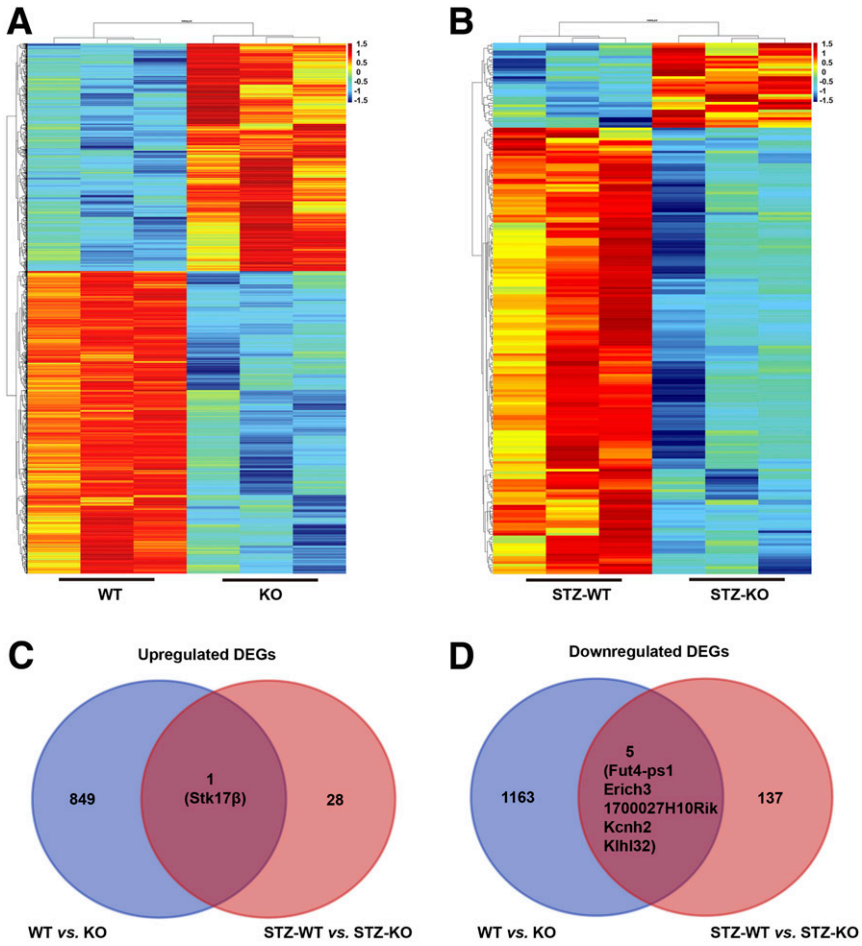

Figure 8—Gene set enrichment analysis comparing isolated islets from HU and/or diabetic mice. Heat maps from mouse isolated islets are shown. Each colored box represents the normalized expression level of a given gene in a particular experimental condition of WT vs. KO (*A*) and STZ-WT vs. STZ-KO (*B*). Red denotes upregulation and blue denotes downregulation according to the color scale. Shared upregulated (*C*) and downregulated (*D*) DEG numbers were enriched in WT vs. KO and in STZ-WT vs. STZ-KO groups. One gene (*Stk17β*) was shared in the upregulated gene set and five genes (*Fut4-ps1*, *Erich3*, *1700027H10Rik*, *Kcnh2*, and *Klhl32*) were shared in the downregulated gene set, with adjusted $P < 0.05$ and absolute fold change >2 (8-week-old WT and KO mice and 11-week-old STZ-WT and STZ-KO mice, $n = 3$ in each group).

nephropathy. Furthermore, the authors of a post hoc analysis in diabetic nephropathy with mean follow-up of 3 years concluded that urate was weakly associated with decline in the glomerular filtration rate (GFR) in patients with type 1 diabetes with overt nephropathy (39). Evidence showed urate may facilitate the development and progression of CKD in people with diabetes (40–42). However, the benefits of urate-lowering are still putative and inconclusive. A post hoc analysis of the Febuxostat Open-Label Clinical Trial of Urate-Lowering Efficacy and Safety Study (FOCUS) with 116 HU patients treated with febuxostat for 5 years found an inverse correlation between urate and estimated (e)GFR and projected an improvement in eGFR of 1 mL/min/1.73 m^2 for every 1 mg/dL decrease in SU (43). In a randomized clinical trial, the authors found a significant association between higher urate and lower GFR ($P = 0.017$), while this association was absent in the allopurinol treatment ($P = 0.61$) (44).

However, the renal status in the above studies was assessed with the eGFR and/or urinary albumin excretion rate, which manifested the glomerular not the tubular function. Despite the current availability of conclusive trial data, Bartáková et al. (45) have recommended 10–15% lower SU cutoff values for people with diabetes to confer protection against kidney disease. In an animal study, Kosugi et al. (34) found that *db/db* mice developed HU and glomerular mesangial expansion (an early feature of diabetic nephropathy). Allopurinol treatment significantly lowered urate levels and reduced tubulointerstitial injury but without amelioration of glomerular lesions in diabetes (34). These results were consistent with our reported data. However, the mixed conclusion of whether lowering SU benefits diabetic nephropathy from Mendelian randomization and clinical and animal studies needs to be carefully explained.

The underlying mechanism of how urate interferes with the function of pancreatic β-cells has not been well

elucidated. Roncal-Jimenez et al. (46) showed that sugar-induced HU likely played a role in the development of diabetes through an effect that included a direct urate effect on islet insulin secretion. Previous studies demonstrated β-cell toxicity of soluble urate via the NF-κB–iNOS–NO signal axis (7). Our research is the first study to elucidate the molecular changes occurring specifically in HU and/or diabetic islets by microarray. The transcriptomic analysis of isolated islets indicates major alterations in shared DEGs with up- and downregulation that might contribute to the accelerated progression of urate-induced cell death. Death-associated protein kinase–related apoptosis-inducing kinase-2 (Drak2), also known as Stk17β, is a serine/threonine kinase that executes its role by apoptosis-related pathways. Stk17β rapidly induces apoptosis in mouse islet β-cells by inflammatory cytokines (47) and free fatty acids (48). Stk17β overexpression, along with the cytokine assaults, has been demonstrated to lead to aggravated apoptosis of β-cells (47), which was consistent with our transcriptomic results (Fig. 8). Mao et al. (47) suggested the inflammatory cytokine/Stk17β/p70S6 kinase pathway seemed to be critical in islet apoptosis. They also demonstrated Stk17β acted through caspase-9 in apoptosis (47). Together with our transcriptomic profiles, these lines of evidence indicate that Stk17β is a potential gene in urate-mediated islet apoptosis of STZ-induced diabetes.

Particularly, reduced levels of TG and unchanged TC levels in *Uox*-KO mice may partially explain the absence of an insulin-resistance phenotype given TG are an independent risk factor for the future development of insulin resistance (49). The decreased TG levels are attributable to sex hormones per se, since it has been reported that testosterone enhances TG in rodents (50) while our HU mice had lower testosterone (data not shown).

Limitations of this study also need to be pointed out. To meet the animal ethic, the mice were euthanized with CO_2, followed by cervical dislocation before islet isolation. CO_2, as an additional stress on the islets, may magnify gene expression differences between KO and WT islets. Although *Uox*-KO mice displayed high SU levels comparable to those observed in adult humans, their germline disruption of *Uox* produced embryonic or postnatal developmental effects such as nephropathy. We also acknowledge this potential caveat that the mice developed kidney disease and urate crystalluria spontaneously, as we previously described (10). To separate whether the impaired glucose tolerance is due to the impaired renal function or to the urate, mice with a conditional and inducible disruption of *Uox* (e.g., tamoxifen-responsive cre mice) may be used to obviate the concern.

In conclusion, the current study demonstrates that urate per se is insufficient to induce diabetes, while it impairs glucose tolerance. For the first time, our research using a constitutive HU model corroborates that high levels of urate predispose mice to diabetes by disrupting β-cell function. Diabetes incidence, β-cell death, or glomerular lesions in diabetes were not reversed by ULT with significance; however, ULT displayed a therapeutic effect on HU-crystal–associated kidney injury and tubulointerstitial damage in diabetic nephropathy. Transcriptomic profiling suggested Stk17β is a urate primacy gene in β-cell apoptosis. We believe that our microarray data specifically from isolated islets of HU mice can serve as a valuable resource for investigators in the field for further exploration of specific genes involved in HU with glycol-metabolic dysfunction.

Acknowledgments. The authors thank pathologists Shihong Shao, Xiangyan Zhang, and Feng Hou (Department of Pathology, the Affiliated Hospital of Qingdao University) for their professional technical support.

Funding. This study was supported by research project grants from the National Key Research and Development Program (2016YFC0903400), the National Science Foundation of China (31900413, 81520108007, and 81770869), the Shandong Province Key Research and Development Program (2018CXGC1207), and the Shandong Province Natural Science Foundation (ZR2018ZC1053).

Duality of Interest. No potential conflicts of interest relevant to this article were reported.

Author Contributions. J.L., Y.H., L.C., Z.L., X.L., H.Z., H.L., W.S., A.J., and Y.W. performed the experiments. J.L., Y.H., H.Y., and C.L. designed the study. J.L., Y.H., X.X., H.Y., and C.L. analyzed and interpreted the data. All authors approved the final version to be published. J.L. and C.L. are the guarantors of this work and, as such, had full access to all the data in the study and take responsibility for the integrity of the data and the accuracy of the data analysis.

References

1. Zhu Y, Pandya BJ, Choi HK. Prevalence of gout and hyperuricemia in the US general population: the National Health and Nutrition Examination Survey 2007-2008. Arthritis Rheum 2011;63:3136–3141

2. Liu H, Zhang XM, Wang YL, Liu BC. Prevalence of hyperuricemia among Chinese adults: a national cross-sectional survey using multistage, stratified sampling. J Nephrol 2014;27:653–658

3. Stamp LK, Wells JE, Pitama S, et al. Hyperuricaemia and gout in New Zealand rural and urban Māori and non-Māori communities. Intern Med J 2013;43:678–684

4. van der Schaft N, Brahimaj A, Wen KX, Franco OH, Dehghan A. The association between serum uric acid and the incidence of prediabetes and type 2 diabetes mellitus: the Rotterdam Study. PLoS One 2017;12:e0179482

5. Kodama S, Saito K, Yachi Y, et al. Association between serum uric acid and development of type 2 diabetes. Diabetes Care 2009;32:1737–1742

6. Sluijs I, Holmes MV, van der Schouw YT, et al.; InterAct Consortium. A Mendelian randomization study of circulating uric acid and type 2 diabetes. Diabetes 2015;64:3028–3036

7. Jia L, Xing J, Ding Y, et al. Hyperuricemia causes pancreatic β-cell death and dysfunction through NF-κB signaling pathway. PLoS One 2013;8:e78284

8. Álvarez-Lario B, Macarrón-Vicente J. Uric acid and evolution. Rheumatology (Oxford) 2010;49:2010–2015

9. Lu J, Dalbeth N, Yin H, Li C, Merriman TR, Wei WH. Mouse models for human hyperuricaemia: a critical review. Nat Rev Rheumatol 2019;15:413–426

10. Lu J, Hou X, Yuan X, et al. Knockout of the urate oxidase gene provides a stable mouse model of hyperuricemia associated with metabolic disorders. Kidney Int 2018;93:69–80

11. Watanabe T, Tomioka NH, Watanabe S, Tsuchiya M, Hosoyamada M. False in vitro and in vivo elevations of uric acid levels in mouse blood. Nucleosides Nucleotides Nucleic Acids 2014;33:192–198

12. Ma PF, Jiang J, Gao C, et al. Immunosuppressive effect of compound K on islet transplantation in an STZ-induced diabetic mouse model. Diabetes 2014;63:3458–3469

13. Do OH, Low JT, Thorn P. Lepr(db) mouse model of type 2 diabetes: pancreatic islet isolation and live-cell 2-photon imaging of intact islets. J Vis Exp 2015;(99): e52632
14. Ramírez-Domínguez M. Isolation of mouse pancreatic islets of Langerhans. Adv Exp Med Biol 2016;938:25–34
15. Juraschek SP, McAdams-Demarco M, Miller ER, et al. Temporal relationship between uric acid concentration and risk of diabetes in a community-based study population. Am J Epidemiol 2014;179:684–691
16. Dehghan A, van Hoek M, Sijbrands EJ, Hofman A, Witteman JC. High serum uric acid as a novel risk factor for type 2 diabetes. Diabetes Care 2008;31:361–362
17. Zhi L, Yuzhang Z, Tianliang H, Hisatome I, Yamamoto T, Jidong C. High uric acid induces insulin resistance in cardiomyocytes in vitro and in vivo. PLoS One 2016;11:e0147737
18. Krishnan E, Pandya BJ, Chung L, Hariri A, Dabbous O. Hyperuricemia in young adults and risk of insulin resistance, prediabetes, and diabetes: a 15-year follow-up study. Am J Epidemiol 2012;176:108–116
19. Dawson J, Wyss A. Chicken or the egg? Hyperuricemia, insulin resistance, and hypertension. Hypertension 2017;70:698–699
20. Wan X, Xu C, Lin Y, et al. Uric acid regulates hepatic steatosis and insulin resistance through the NLRP3 inflammasome-dependent mechanism. J Hepatol 2016;64:925–932
21. Holter MM, Garibay D, Lee SA, et al. Hepatocyte p53 ablation induces metabolic dysregulation that is corrected by food restriction and vertical sleeve gastrectomy in mice. FASEB J 2020;34:1846–1858
22. Pfister R, Barnes D, Luben R, et al. No evidence for a causal link between uric acid and type 2 diabetes: a Mendelian randomisation approach. Diabetologia 2011;54:2561–2569
23. Nakagawa T, Hu H, Zharikov S, et al. A causal role for uric acid in fructose-induced metabolic syndrome. Am J Physiol Renal Physiol 2006;290:F625–F631
24. Baldwin W, McRae S, Marek G, et al. Hyperuricemia as a mediator of the proinflammatory endocrine imbalance in the adipose tissue in a murine model of the metabolic syndrome. Diabetes 2011;60:1258–1269
25. Cicerchi C, Li N, Kratzer J, et al. Uric acid-dependent inhibition of AMP kinase induces hepatic glucose production in diabetes and starvation: evolutionary implications of the uricase loss in hominids. FASEB J 2014;28:3339–3350
26. Butler AE, Janson J, Bonner-Weir S, Ritzel R, Rizza RA, Butler PC. Beta-cell deficit and increased beta-cell apoptosis in humans with type 2 diabetes. Diabetes 2003;52:102–110
27. Johnson RJ, Merriman T, Lanaspa MA. Causal or noncausal relationship of uric acid with diabetes. Diabetes 2015;64:2720–2722
28. Takir M, Kostek O, Ozkok A, et al. Lowering uric acid with allopurinol improves insulin resistance and systemic inflammation in asymptomatic hyperuricemia. J Investig Med 2015;63:924–929
29. Ogino K, Kato M, Furuse Y, et al. Uric acid-lowering treatment with benzbromarone in patients with heart failure: a double-blind placebo-controlled crossover preliminary study. Circ Heart Fail 2010;3:73–81
30. Niu SW, Chang KT, Ta A, et al. Decreased incidence of diabetes in patients with gout using benzbromarone. Rheumatology (Oxford) 2018;57:1574–1582
31. Cai HY, Wang T, Zhao JC, et al. Benzbromarone, an old uricosuric drug, inhibits human fatty acid binding protein 4 in vitro and lowers the blood glucose level in db/db mice. Acta Pharmacol Sin 2013;34:1397–1402
32. Previte DM, Piganelli JD. Reactive oxygen species and their implications on CD_4^+ T cells in type 1 diabetes. Antioxid Redox Signal 2018;29:1399–1414
33. Gilbert RE, Cooper ME. The tubulointerstitium in progressive diabetic kidney disease: more than an aftermath of glomerular injury? Kidney Int 1999;56:1627–1637
34. Kosugi T, Nakayama T, Heinig M, et al. Effect of lowering uric acid on renal disease in the type 2 diabetic *db*/*db* mice. Am J Physiol Renal Physiol 2009;297: F481–F488
35. Isono M, Cruz MC, Chen S, Hong SW, Ziyadeh FN. Extracellular signal-regulated kinase mediates stimulation of TGF-beta1 and matrix by high glucose in mesangial cells. J Am Soc Nephrol 2000;11:2222–2230
36. Testa A, Mallamaci F, Spoto B, et al. Association of a polymorphism in a gene encoding a urate transporter with CKD progression. Clin J Am Soc Nephrol 2014;9: 1059–1065
37. Ahola AJ, Sandholm N, Forsblom C, Harjutsalo V, Dahlström E, Groop PH; FinnDiane Study Group. The serum uric acid concentration is not causally linked to diabetic nephropathy in type 1 diabetes. Kidney Int 2017;91:1178–1185
38. Liu J, Zhang H, Dong Z, et al. Mendelian randomization analysis indicates serum urate has a causal effect on renal function in Chinese women. Int Urol Nephrol 2017;49:2035–2042
39. Pilemann-Lyberg S, Lindhardt M, Persson F, Andersen S, Rossing P. Serum uric acid and progression of diabetic nephropathy in type 1 diabetes. J Diabetes Complications 2018;32:470–473
40. Jalal DI, Rivard CJ, Johnson RJ, et al. Serum uric acid levels predict the development of albuminuria over 6 years in patients with type 1 diabetes: findings from the Coronary Artery Calcification in Type 1 Diabetes study. Nephrol Dial Transplant 2010;25:1865–1869
41. Hovind P, Rossing P, Tarnow L, Johnson RJ, Parving HH. Serum uric acid as a predictor for development of diabetic nephropathy in type 1 diabetes: an inception cohort study. Diabetes 2009;58:1668–1671
42. De Cosmo S, Viazzi F, Pacilli A, et al.; AMD-Annals Study Group. Serum uric acid and risk of CKD in type 2 diabetes. Clin J Am Soc Nephrol 2015;10:1921–1929
43. Whelton A, Macdonald PA, Zhao L, Hunt B, Gunawardhana L. Renal function in gout: long-term treatment effects of febuxostat. J Clin Rheumatol 2011;17:7–13
44. Pilemann-Lyberg S, Persson F, Frystyk J, Rossing P. The effect of uric acid lowering treatment on albuminuria and renal function in Type 1 diabetes: a randomized clinical trial. Diabet Med 2018;35:392–393
45. Bartáková V, Kuricová K, Pácal L, et al. Hyperuricemia contributes to the faster progression of diabetic kidney disease in type 2 diabetes mellitus. J Diabetes Complications 2016;30:1300–1307
46. Roncal-Jimenez CA, Lanaspa MA, Rivard CJ, et al. Sucrose induces fatty liver and pancreatic inflammation in male breeder rats independent of excess energy intake. Metabolism 2011;60:1259–1270
47. Mao J, Luo H, Han B, Bertrand R, Wu J. Drak2 is upstream of p70S6 kinase: its implication in cytokine-induced islet apoptosis, diabetes, and islet transplantation. J Immunol 2009;182:4762–4770
48. Mao J, Luo H, Wu J. Drak2 overexpression results in increased beta-cell apoptosis after free fatty acid stimulation. J Cell Biochem 2008;105:1073–1080
49. Kroetsch AM, Sahin E, Wang HY, Krizman S, Roberts CJ. Relating particle formation to salt- and pH-dependent phase separation of non-native aggregates of alpha-chymotrypsinogen A. J Pharm Sci 2012;101:3651–3660
50. Senmaru T, Fukui M, Okada H, et al. Testosterone deficiency induces markedly decreased serum triglycerides, increased small dense LDL, and hepatic steatosis mediated by dysregulation of lipid assembly and secretion in mice fed a high-fat diet. Metabolism 2013;62:851–860